BioMetals (2005) 18:295–303
DOI 10.1007/s10534-005-3685-y

Zinc–ligand interactions modulate assembly and stability of the insulin hexamer – a review

Michael F. Dunn*
Department of Biochemistry, University of California, Riverside, CA 92521, USA;
**Author for correspondence (E-mail: michael.dunn@ucr.edu)*

Key words: allosteric transitions, calcium, hexamer, insulin, zinc

Abstract

Zinc and calcium ions play important roles in the biosynthesis and storage of insulin. Insulin biosynthesis occurs within the β-cells of the pancreas via preproinsulin and proinsulin precursors. In the golgi apparatus, proinsulin is sequestered within Zn^{2+}- and Ca^{2+}-rich storage/secretory vesicles and assembled into a Zn^{2+} and Ca^{2+} containing hexameric species, $(Zn^{2+})_2(Ca^{2+})(Proin)_6$. In the vesicle, $(Zn^{2+})_2(Ca^{2+})(Proin)_6$ is converted to the insulin hexamer, $(Zn^{2+})_2(Ca^{2+})(In)_6$, by excision of the C-peptide through the action of proteolytic enzymes. The conversion of $(Zn^{2+})_2(Ca^{2+})(Proin)_6$to $(Zn^{2+})_2(Ca^{2+})(In)_6$ significantly lowers the solubility of the hexamer, causing crystallization within the vesicle. The $(Zn^{2+})_2(Ca^{2+})(In)_6$ hexamer is an allosteric protein that undergoes ligand-mediated interconversion among three global conformation states designated T_6, T_3R_3 and R_6. Two classes of allosteric sites have been identified; hydrophobic pockets (3 in T_3R_3 and 6 in R_6) that bind phenolic ligands, and anion sites (1 in T_3R_3 and 2 in R_6) that bind monovalent anions. The allosteric states differ widely with respect to the physical and chemical stability of the insulin subunits. Fusion of the vesicle with the plasma membrane results in the expulsion of the insulin crystals into the intercellular fluid. Dissolution of the crystals, dissociation of the hexamers to monomer and transport of monomers to the liver and other tissues then occurs via the blood stream. Insulin action then follows binding to the insulin receptors. The role of Zn^{2+} in the assembly, structure, allosteric properties, and dynamic behavior of the insulin hexamer will be discussed in relation to biological function.

Introduction

This article presents a mini-review of the roles played by divalent metal ions in the structure and function of the insulin hexamer emphasizing a retrospective of studies performed in collaboration with the author's laboratory. Owing to space constraints, this review gives limited coverage of the large body of elegant and excellent work carried out by many other laboratories. The author apologizes for these oversights.

Biosynthesis of insulin, assembly, and storage in vesicles

The biosynthesis and storage of insulin is strongly modulated by the binding of zinc and calcium ions (Howell *et al.* 1975; Sudmeier *et al.* 1981). Insulin biosynthesis occurs within the β-cells of the pancreas via the precursors preproinsulin and proinsulin (Ashcroft & Ashcroft 1992). Upon cleavage of the signal sequence from preproinsulin, the proinsulin formed is transported to the golgi where it is sequestered within Zn^{2+}- and Ca^{2+}-rich storage/secretory vesicles and assembled into a Zn^{2+} and Ca^{2+} containing hexameric species designated herein as $(Zn^{2+})_2(Ca^{2+})(Proin)_6$. In the secretory vesicle, excision of the C-peptide by trypsin- and carboxypeptidase-like enzymes converts $(Zn^{2+})_2(Ca^{2+})(Proin)_6$ to the insulin hexamer, $(Zn^{2+})_2(Ca^{2+})(In)_6$ (Figure 1a). C-peptide removal significantly alters the solubility of the hexamer, causing crystallization of $(Zn^{2+})_2(Ca^{2+})(In)_6$

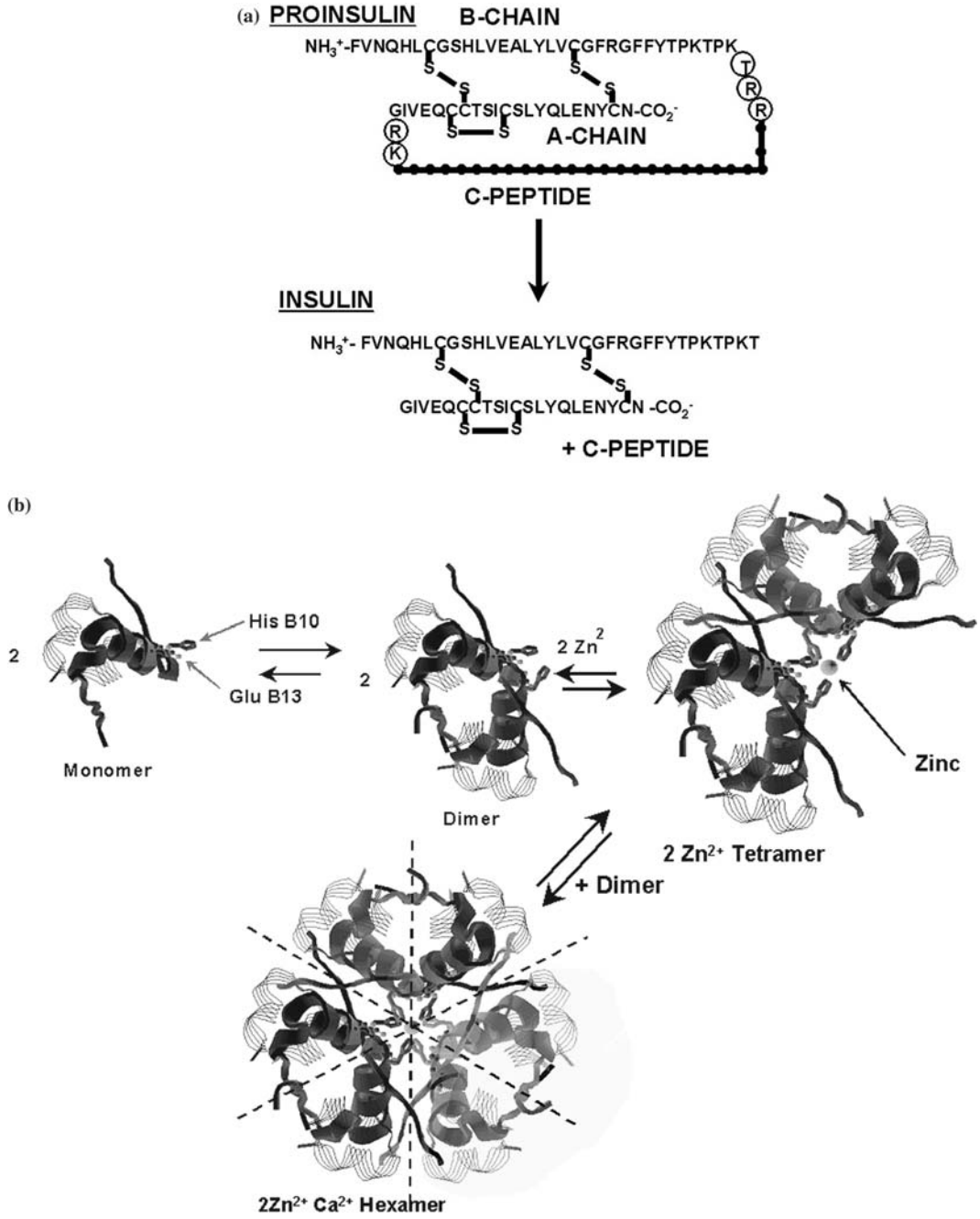

Figure 1. (a) Scheme depicting the conversion of proinsulin to insulin and the C-peptide through the action of the trypsin-like and carboxypeptidase-like enzymes of the secretory vesicle. (b) Pathway for the assembly of the T_6 insulin hexamer. Structures are viewed along the hexamer 3-fold symmetry axis. The three pseudo 2-fold symmetry axes of the hexamer are shown as dashed lines (structures created from 4INS.PDB, Baker *et al.* 1988).

within the vesicle (Ashcroft & Ashcroft 1992). The $(Zn^{2+})_2(Ca^{2+})(In)_6$ hexamer is an inactive, storage form that must be converted to insulin monomer for biological activity.

Hexamer assembly

The assembly pathway of the insulin hexamer (Figure 1b) is proposed to involve the formation

of insulin dimers followed by the combination of two dimers with two zinc ions to give a $(Zn^{2+})_2(In)_4$ tetramer which then combines with another dimeric unit to give the insulin hexamer (Coffman & Dunn 1988; Kadima *et al.* 1992). Monomeric and dimeric insulins have no strong chelating sites for divalent metal ions. The insulin tetramer has partially formed Zn^{2+} and Ca^{2+} sites consisting of two His B10 side chains at each Zn^{2+} site, and four GluB13 side chains at the Ca^{2+} site. Consequently, Zn^{2+} and Ca^{2+} binding likely becomes significant only at the tetrameric stage of assembly. The addition of the third insulin dimer completes the assembly of the His B10 Zn^{2+} sites and the Ca^{2+} site. It is presumed that assembly of the proinsulin hexamer occurs by a similar path.

Biological function of the hexamer as the storage form

The biological function of the hexamer in the biosynthesis, assembly and storage of insulin within the secretory vesicles is not clearly established. Extrapolation based on the physical and chemical properties of the insulin hexamer suggest that hexamer formation likely serves the following functions: (a) The Zn^{2+}- and Ca^{2+}-mediated assembly of the proinsulin hexamer creates a structure that protects some portions of the polypeptide chain from proteolytic cleavage by burial within the subunit interfaces of a soluble hexamer, while leaving the C-peptide segment of proinsulin exposed on the hexamer surface to the action of the trypsin- and carboxypeptidase-like processing enzymes. (b) The change in solubility on conversion of the proinsulin hexamer to the insulin hexamer and consequent crystallization of the insulin hexamer provides further protection of newly formed insulin chains and segregates proinsulin from insulin as the conversion to insulin occurs. (c) *In vitro* studies have shown that the insulin hexamer is much more stable to chemical and/or physical degradation than the insulin monomer. Consequently, hexamer formation and crystallization stabilizes insulin, preventing degradation within the storage vesicle.

Insulin was first introduced for treatment of insulin-dependent diabetes mellitus in the early 1920s (Banting & Best 1922). Owing to their superior stability, hexameric forms of insulin now are widely used in the formulation of pharmaceutical preparations. These insulin formulations are enormously stabilized by the binding of allosteric ligands at two loci, the phenolic pockets, and the His B10 Zn^{2+} sites.

Secretion of insulin via exocytosis

The exocytosis of insulin from the β-cells of the pancreas in response to elevated levels of blood glucose involves fusion of the plasma membrane of the storage vesicle with the cell membrane. When this occurs with vesicles containing a crystal of the insulin hexamer, the crystal is released from the cell into the intercellular space where it dissolves to give insulin monomers. It is estimated that insulin released from the pancreas reaches the liver within about 10 s; hence if biologically active insulin is to be presented to liver cell receptors, then dissolution of the crystals and dissociation of hexamer to monomer must occur within this time frame. Insulin monomers then are transferred into the blood stream and transported to the liver where binding of insulin to liver cell receptors triggers the uptake of glucose from the blood. The dynamics of this sequence of events presents interesting questions about the mechanism of crystal dissolution and hexamer dissociation. Some hints concerning likely mechanisms arise from the structural properties and conformational dynamics of the insulin hexamer. These subjects will be discussed below.

Insulin hexamer conformation states; T_6, T_3R_3 and R_6

In 1989, Kaarsholm *et al.* (1989) recognized that the $(Zn^{2+})_2(Ca^{2+})(In)_6$ hexamer is an allosteric protein that undergoes ligand-mediated interconversion among three global conformation states designated T_6, T_3R_3 and R_6. Structures of the T_6 and R_6 states are compared in Figure 2a and b. In subsequent investigations, two classes of allosteric sites have been identified and characterized. These consist of hydrophobic pockets (3 in T_3R_3 and 6 in R_6) that bind phenolic ligands (e.g., phenol, resorcinol, cresol) (Figure 2d), and anion sites (1 in T_3R_3 and 2 in R_6) (Figure 2f) that bind monovalent anions (e.g., halides, pseudo halides, and organic carboxylates).

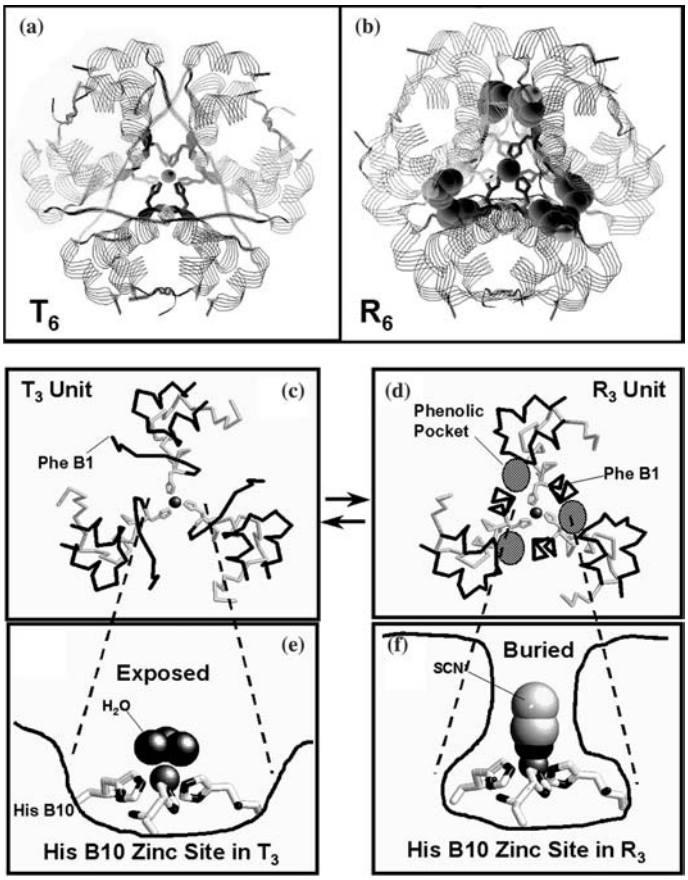

Figure 2. Hexamer symmetry and the binding of allosteric ligands. (a) and (b) are ribbon drawings of the T_6 (4INS.PDB, Baker *et al.* 1988) and R_6 (1EV6.PDB, Smith *et al.* 2000) insulin hexamers viewed along the 3-fold hexamer symmetry axis. His B10 side chains in (a) and (b) are shown in stick representation, the six *m*-cresol ligands bound to the R_6 phenolic pockets in (b) are shown in space filling representation (1EV6.PDB, Smith *et al.* 2000). (c) and (d) show T_3 and R_3 units, respectively, of the hexamer in backbone representation. His B10 side chains are shown in stick representation and the Zn^{2+} ions are shown as black balls. The ~30 Å shift of PheB1 in the coil-to-helix allosteric transition is indicated in (c) and (d), phenolic pockets are indicated as cross-hatched ellipsoids in (d). (e) and (f) are cartoons that depict the octahedral to tetrahedral coordination geometry change at the His B10 site as T_3 (e) is converted to R_3 in the SCN^- complex (f). Zn^{2+} is shown coordinated to three His B10 imidazole groups and to three waters in (e) or to SCN^- in (f) (structure drawn from 2TCI.PDB, Whittingham *et al.* 1995). Solid lines represent the protein surface, of an exposed metal site in (e) and a buried site in (f).

The transition from a T_3 unit of the hexamer to an R_3 unit (Figure 2c–f) involves the conversion of residues 1–9 of the insulin B-chain from an extended conformation to -helix (Smith *et al.* 1984; Derewenda *et al.* 1989; Smith & Dodson 1992a, b; Ciszak & Smith 1994). This transformation gives a 3-helix bundle aligned along the hexamer 3-fold symmetry axis that creates an amphiphatic site involving the His B10 zinc ion (Figures 2f and 3a and b), and forms hydrophobic pockets located at the interfaces between R-state subunits that bind phenolic ligands (Figures 2b, d and 3c). Interconversion among these three allosteric forms can be modulated by the binding of phenol and derivatives of phenol to the hydrophobic pockets (the phenolic pockets) of the R-state species, and by the binding of monovalent anions including halides, pseudo halides, and organic carboxylates coordinated to the zinc ions at the His B10 sites (Kaarsholm *et al.* 1989; Roy *et al.* 1989; Brader & Dunn 1991; Brader *et al.* 1991; Choi *et al.* 1993; Brzovic *et al.* 1994; Huang *et al.* 1997). The pockets within an R_3 unit are ~20 Å distant from each other, the two zinc sites within a hexamer are ~16 Å distant from each other, and the closest distance between a phenolic pocket and a His B10 site is approximately 6–8 Å. The Ca^{2+} site is located near the center of the hexamer, where the six

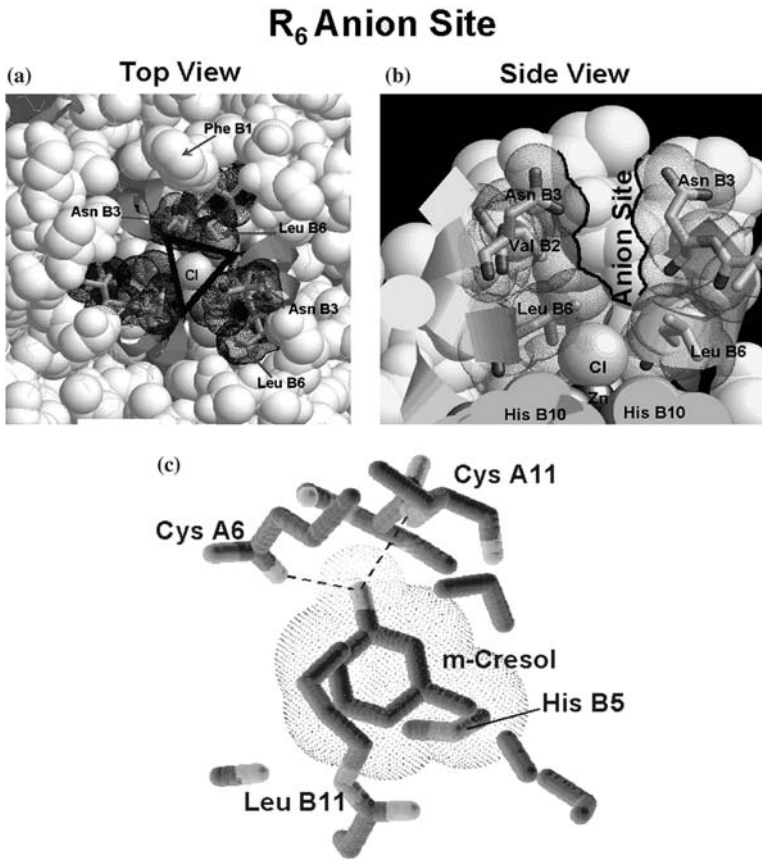

Figure 3. Structures of the allosteric sites. (a) and (b): top and side views, respectively, of the His B10 anion site with chloride ion coordinated to Zn^{2+}. The triangle in (a) illustrates the 3-fold symmetry of the site. In (a) and (b), the protein is shown in space fill representation, the residues that form the binding site surface are shown in stick representation with the van der Waals dot surface (black). In (b), the structure is cut away to reveal the anion site. (c) Stick representations of the residues within 5 Å of *m*-cresol with its van der Waals surface (black dots) at the phenolic pocket. Dashed lines indicate H-bonds between the *m*-cresol hydroxyl and the carbonyl of CysA6 and the NH of CysA11. Structures prepared from 1EV6.PDB (Smith *et al.* 2000).

B13 glutamate carboxyl groups are positioned as pairs about the center of a ~12 Å diameter cavity (Figure 4). This site was discovered in a series of $^{113}Cd^{2+}$ NMR studies by Sudmeier *et al.* (1981) (Figure 4A). They showed that $^{113}Cd^{2+}$ could be substituted into the His B10 Zn^{2+} sites and into a third, previously unrecognized site. Ca^{2+} was shown to be effective in displacing $^{113}Cd^{2+}$ from the new site but not from the His B10 Zn^{2+} sites, identifying it as a Ca^{2+} site. X-ray diffraction studies of the Cd^{2+} and Pb^{2+} hexamer derivatives showed these metal ions bind to the six GluB13 carboxylates at three closely spaced symmetry-related positions at the center of the hexamer, each exhibiting 1/3 occupancy (Figure 4B). Owing to the close spacing of these sites, this cavity can accommodate only a single divalent metal ion at any time, hence there is a random population of the three positions throughout the crystal lattice. A model for the Ca^{2+} complex is shown in Figure 4C in which pairs of GluB13 carboxylates along with two water molecules coordinate each Ca^{2+}. The binding of Ca^{2+} contributes stability to the insulin hexamer (Storm & Dunn 1985).

In the absence of allosteric ligands, the insulin hexamer exists predominantly in the T_6 state (Figure 2a). The T_3R_3 state can be stabilized by the binding of thiocyanate ion (Kaarsholm *et al.* 1989; Brader *et al.* 1991; Whittingham *et al.* 1995) or certain phenolic ligands (Dodson *et al.* 1993; Bloom *et al.* 1995, 1997a, b, 1998), and the R_6 state (Figure 2b) is stabilized by the binding of the combination of phenolic ligands and monovalent anions (Derewenda *et al.* 1989; Roy *et al.* 1989;

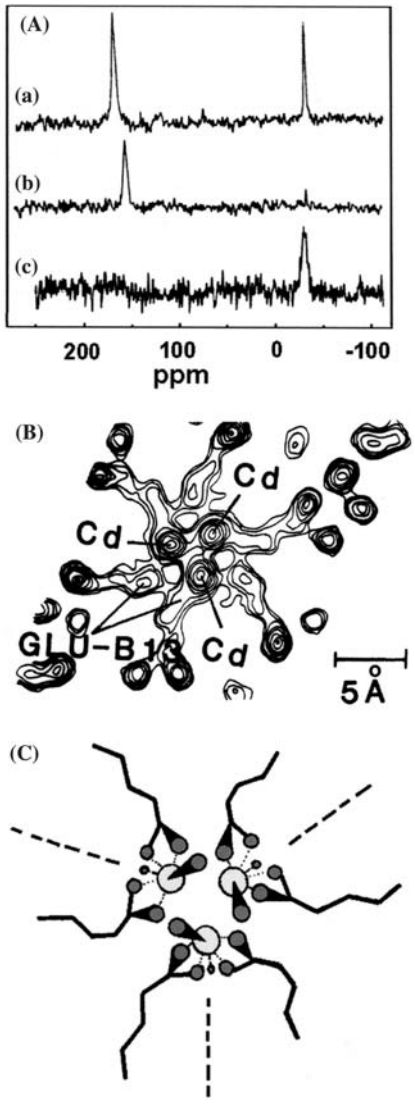

Figure 4. Evidence for the Ca^{2+} site from Cd^{2+} substitution. (A) $^{113}Cd^{2+}$ NMR spectra: (a) the T_6 hexamer with $^{113}Cd^{2+}$ substituted into the GluB13 site (1) and the His B10 sites (2). (b) $^{113}Cd^{2+}$ is displaced from the GluB13 site by Ca^{2+}. (c) $^{113}Cd^{2+}$ is displaced from the His B10 sites by Zn^{2+} (Sudmeier *et al.* 1981). (B) Electron density map of the GluB13 site substituted with Cd^{2+} viewed along the 3-fold molecular symmetry axis. Notice the three symmetry-related Cd^{2+} positions (1/3 occupancy each), and the disordered densities of the GluB13 side chains. (C) Model depicting two GluB13 carboxylates and two waters (small circles) to each Cd position (large circles) (Hill *et al.* 1991).

Brader & Dunn 1991; Brader *et al.* 1991; Smith & Dodson 1992a, b; Choi *et al.* 1993; Brzovic *et al.* 1994; Huang *et al.* 1997; Olsen *et al.* 2003). The T_6 and R_6 species possess one 3-fold and three pseudo 2-fold axes of symmetry. The pseudo 2-fold axes of symmetry have their origins in a slight asymmetry in the dimeric units of T_6 (Blundell *et al.* 1972; Baker *et al.* 1988) and R_6 (Derewenda *et al.* 1989; Smith & Dodson 1992a, b). Owing to the large difference in B-chain conformations within a TR dimeric unit, the T_3R_3 species retains only a 3-fold symmetry axis.

The allosteric states differ widely with respect to the physical and chemical stability of the insulin subunits within each hexamer, exhibiting the following stability order: $R_6 > > T_3R_3 > > T_6$ (Rahuel-Clermont *et al.* 1997). The relationship of the binding sites and allosteric properties of the insulin hexamer to the storage and secretion of insulin is not understood, and it is not known which allosteric state is crystallized within the vesicles. For teleological reasons, we speculate that the hexamers within storage vesicles are either T_3R_3 or R_6 for two simple reasons: (a) Why else would the sites for the allosteric ligands be preserved through evolution in virtually all vertebrate species? (b) The much greater stabilities of T_3R_3 and R_6 compared to T_6 imply a significant role of the R-state species in storage. While the evidence is clear for the existence of the allosteric sites in the T_3R_3 and R_6 hexamers from many species, what remains unclear are the identities of the putative *in vivo* allosteric ligands.

Anatomy of the insulin allosteric binding sites

The phenolic pockets of T_3R_3 and R_6 hexamers are created by a coil-to-helix T- to R-conformational transition which causes a ~30 Å dislocation of the PheB1 ring (Figure 2). These pockets extend from the center of the hexamer at GluB13 to just below the surface. Phenol and derivatives of phenol bind by forming two H-bonds between the phenolic hydroxyl and the carbonyl oxygen of CysA6 and the amide NH of CysA11 at one end of the pocket (Figure 3c). This H-bonding appears essential for binding. Additional weak bonding interactions consist of van der Waals interactions. These pockets can accommodate phenol, *meta*-cresol, resorcinol, and the phenol analogues 2,6- and 2,7-dihydroxynaphthalene (2,6- and 2,7-DHN) (Table 1). In the 2,6- and 2,7-DHN complexes, an additional H-bond likely is formed between the second hydroxyl group and a GluB13 carboxylate at the other end of the pocket.

Table 1. R-State allosteric ligands of the insulin hexamer.

Typical Phenolic Pocket Ligands	Typical HisB10 Anion Site Ligands
 Phenol	Halides, pseudo halides
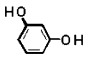 Resorcinol	Organic carboxylates:
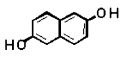 2,6-Dihydroxy-naphthalene	 p-Aminobenzoate
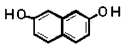 2,7-Dihydroxy-naphthalene	 3-Nitro-4-hydroxy-benzoate
	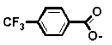 4-CF_3-benzoate
	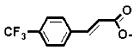 4-CF_3-*trans*-cinnamate

The His B10 anion sites are also formed by the coil-to-helix T- to R-state transformation (Figure 2). Conversion of a T_3 unit to an R_3 unit is accompanied by the conversion of each His B10 zinc ion from an octahedral Zn^{2+} N_3O_3 complex (N is His B10, O is H_2O) (Figure 2e) to a distorted tetrahedral Zn^{2+} N_3L complex (where L is a monovalent anion) (Figure 2f) (Derewenda *et al.* 1989; Smith & Dodson 1992a, b; Ciszak & Smith 1994; Whittingham *et al.* 1995; Brader *et al.* 1997). The ~12 Å tunnel from the surface to Zn^{2+} created by the three helix bundle (Figure 3) provides a 3-fold symmetric amphiphatic surface that accommodates monoanions ranging in structure from halides and pseudo halides to organic carboxylates as large as *meta*- or *para*-substituted benzoates or substituted cinnamates (Table 1) (Brader *et al.* 1991, 1997; Huang *et al.* 1997; Olsen *et al.* 2003).

Positive and negative cooperativity and half-site reactivity: insulin and the SMB model

The interconversion among the T_6, T_3R_3 and R_6 allosteric states conveys positive and negative cooperativity and apparent half-site ligand binding activity to the insulin hexamer. Consequently, the insulin hexamer is an important paradigm for the study of allostery. Bloom *et al.* (1995, 1997a, b, 1998) have established that insulin allosteric behavior is well described by the allosteric model of Seydoux, Malhotra, and Bernhard (Seydoux *et al.* 1974; the SMB model). The SMB model, when tailored to the insulin hexamer (Figure 5), postulates that the allosteric behavior is the consequence of two interrelated allosteric transitions designated L_A^0 and L_B^0 (Figure 5) involving three allosteric conformation states (T_6, T_3R_3 and R_6) with two classes of allosteric ligand binding sites (the phenolic pockets and the His B10 anion sites). These allosteric sites exist only in the T_3R_3 and R_6 states. Owing to slight differences in the conformations of the phenolic pockets of T_3R_3 and R_6, the model requires different dissociation constants, K_R^0 and K_R, respectively, for binding phenolic ligands to T_3R_3 and to R_6. Bloom *et al.* (1995, 1997a, b, 1998) have demonstrated the applicability of this model by quantification of the binding isotherms (Figure 6) for a wide variety of ligands for wild-type and mutant Zn^{2+}- and Co^{2+}-substituted insulin hexamers.

Hexamer stability and the allosteric state of insulin

The insulin monomer is far more susceptible than the hexamer to thermal and mechanical (fibrillation) denaturation and to chemical degradation (e.g., deamidation, disulfide bridge cleavage, and covalent dimerization by reaction of the B chain amino terminus with Asn or Gln residues). R_6 species are generally much more stable than T_3R_3 species, which are much more stable than T_6 species. Rahuel-Clermont *et al.* (1997) have quantified stability by using a kinetic probe to measure the effects of homotropic and heterotropic effectors on

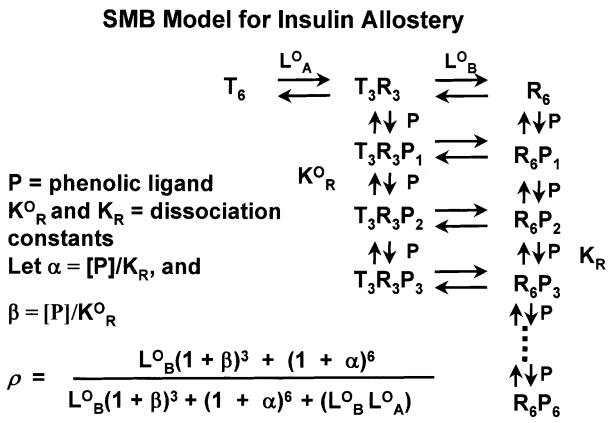

Figure 5. The allosteric model of Seydoux, Malhotra, and Bernhard (SMB model) tailored to the subunit symmetry properties of the T_6, T_3R_3 and R_6 hexamers (Bloom *et al.* 1995). The equation for the fraction of R-state subunits, ρ, is indicated. The model consists of preexisting T_6, T_3R_3 and R_6 allosteric states with binding of allosteric ligand (P) only to the T_3R_3 and R_6 states. Structural differences in the phenolic pockets of T_3R_3 and R_6, require separate dissociation constants (K^0_R and K_R) for P binding.

the dissociation kinetics of the Zn^{2+} and Co^{2+} insulin hexamer complexes. The release of the His B10 divalent metal ion and dissociation of the hexamer is limited by the T_3R_3 to T_6 or R_6 to T_3R_3 conformational transition steps and the dissociation of one anionic ligand, or one anionic ligand and three phenolic ligand molecules, respectively, for T_3R_3 and R_6. Since the activation energies of these steps are dominated by the ground state stabilization energy of the R-state species, the kinetic stabilization of the hexamer toward dissociation is linked to the thermodynamic stabilization of the hexamer. The mass action effect of anion binding and, especially, of phenolic ligand binding provides the major mechanism of stabilization. Stabilization correlates with ligand affinity: the tighter the binding, the greater the stabilization.

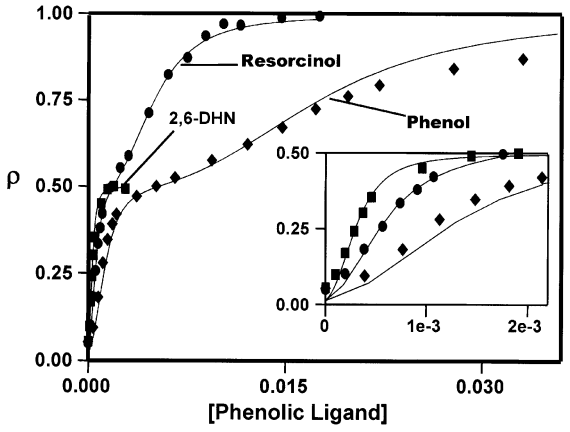

Figure 6. Titrations showing the dependence of ρ (Figure 5) on phenolic ligand concentration. Binding curves: phenol (diamonds), resorcinol (circles) and 2,6-dihydroxynaphthalene (2,6-DHN) (squares). The inset shows the sigmoidal nature of the initial portion of the binding curves. The phenol and resorcinol curves show inflections at $\rho \sim 0.5$, the 2,6-DHN curve tends to saturate at $\rho = 0.5$ (giving apparent half-site reactivity) (from Bloom *et al.* 1997a).

Speculations on the dissolution of insulin crystals and dissociation of the hexamer during exocytosis

The superior stability properties of the T_3R_3 and R_6 hexameric states imply that crystalline hexamers stored in secretory vesicles are either T_3R_3 or R_6. Hence, we speculate that when an insulin crystal is expelled from a β-cell, crystal dissolution and hexamer dissociation are triggered by three events: (a) the change in pH that the crystal experiences upon transfer from the vesicle to the intercellular milieu. This pH change increases the solubility of insulin, and favors dissolution of the crystal. (b) The loss of ligands due to dilution when the crystal is transferred from the vesicle to the intercellular space. Dilution promotes dissociation of the allosteric ligands, and favors switching of the insulin conformation from R-state to T-state. (c) An endogenous chelator removes the His B10 Zn^{2+} ions, favoring dissociation of hexamer to monomer. These events speed dissolution conversion of the crystal to insulin monomer.

Acknowledgements

I thank Niels Kaarsholm for the central role he has played as a collaborator in many of our publilcations, and I also grateful for the generous support of this work by the NIH, the NSF and Novo Nordisk.

References

Ashcroft FM, Ashcroft SJH. 1992 Insulin Molecular Biology to Pathology. New York: Oxford University Press 5–92.

Baker EN, Blundell TL, Cutfield JF, *et al*. 1988 The structure of 2Zn pig insulin crystals at 1.5 Å resolution. *Phil Trans Roy Soc* (London) *B* **319**, 369–456.

Banting FG, Best CH. 1922 Pancreatic extracts. *J Lab Clin Med* **7**, 464–472.

Bloom CR, Choi WE, Brzovic PS, Ha JJ, Huang ST, Kaarsholm NC, Dunn MF. 1995 Ligand binding to wild-type and E-B13Q mutant insulins; A three-state allosteric model system showing half-site reactivity. *J Mol Biol* **245**, 324–330.

Bloom CR, Heymann R, Kaarsholm NC, Dunn MF. 1997a Binding of 2,6- and 2,7-dihydroxynaphthalene to wild-type and E-B13Q insulins: Dynamic, equilibrium and molecular modeling investigations. *Biochemistry* **36**, 12746–12758.

Bloom CR, Kaarsholm NC, Ha JJ, Dunn MF. 1997b Half-site reactivity, negative cooperativity, and positive cooperativity: Quantitative considerations of a plausible model. *Biochemistry* **36**, 12759–12765.

Bloom CR, Wu N, Dunn A, Kaarsholm NC, Dunn MF. 1998 Comparison of the allosteric properties of the Co(II) and Zn(II) substituted insulin hexamers. *Biochemistry* **37**, 10937–10944.

Blundell T, Dodson G, Hodgkin D, Mercola D. 1972 Insulin: The structure in the crystal and its reflection in chemistry and biology. *Adv Protein Chem* **26**, 279–402.

Brader ML, Dunn MF. 1991 Insulin hexamers: New conformations and applications. *Trends Biochem Sci* **16**, 341–345.

Brader ML, Kaarsholm NC, Harnung SE, Dunn MF. 1997 Ligand perturbation on a pseudotetrahedral Co(II)(His)3L site. A magnetic circular dichroism study of the Co(II)-substituted insulin hexamer. *J Biol Chem* **272**, 1088–1094.

Brader ML, Kaarsholm NC, Lee RW-K, Dunn MF. 1991 Characterization of the R-state insulin hexamer and its derivatives. The hexamer is stabilized by heterotropic ligand binding interactions. *Biochemistry* **30**, 6636–6645.

Brzovic PS, Choi WE, Borchardt D, Kaarsholm NC, Dunn MF. 1994 Structural asymmetry and half-site reactivity in the T to R allosteric transition of the insulin hexamer. *Biochemistry* **33**, 13057–13069.

Choi WE, Brader ML, Aguilar V, Kaarsholm NC, Dunn MF. 1993 The allosteric transition of the insulin hexamer is modulated by homotropic and heterotropic interactions. *Biochemistry* **32**, 11638–11645.

Ciszak E, Smith GD. 1994 Crystallographic evidence for dual coordination around zinc in the T_3R_3 human insulin hexamer. *Biochemistry* **33**, 1512–1517.

Coffman FD, Dunn MF. 1988 Insulin–metal ion interactions. The binding of divalent cations to insulin hexamers and tetramers and the assembly of insulin hexamers. *Biochemistry* **27**, 6179–6187.

Derewenda U, Derewenda Z, Dodson EJ, *et al*. 1989 Phenol stabilizes more helix in a new symmetrical zinc insulin hexamer. *Nature* **338**, 594–596.

Hill CP, Dauter Z, Dodson EJ, Dodson GG, Dunn MF. 1991 X-ray structure of an unusual Ca^{2+} site and the roles of Zn^{2+} and Ca^{2+} in the assembly, stability, and storage of the insulin hexamer. *Biochemistry* **30**, 919–924.

Howell SL, Montague W, Tyhurst M. 1975 Ca distribution in islets of Langerhans. *J Cell Sci* **19**, 395–409.

Huang ST, Choi WE, Bloom CR, Leuenberger M, Dunn MF. 1997 Carboxylate ions are strong allosteric ligands for the HisB10 sites of the R-state insulin hexamer. *Biochemistry* **36**, 9878–9888.

Kaarsholm NC, Ko H-C, Dunn MF. 1989 Comparison of solution structural flexibility and zinc binding domains for insulin, proinsulin and mini-proinsulin. *Biochemistry* **28**, 4427–4435.

Kadima W, Roy M, Lee RW-K, Kaarsholm NC, Dunn MF. 1992 Mechanisms of stabilization of the insulin hexamer through allosteric ligand interactions. *J Biol Chem* **267**, 8963–8970.

Olsen HB, Leuenberger-Fisher MR, Kadima W, Borchardt D, Kaarsholm NC, Dunn MF. 2003 Structural signatures of the complex formed between 3-nitro-4-hydroxybenzoate and the Zn(II)-substituted R_6 insulin hexamer. *Protein Sci* **12**, 1902–1913.

Rahuel-Clermont S, French CA, Chou CI, Kaarsholm NC, Dunn MF. 1997 Mechanisms of stabilization of the insulin hexamer through allosteric ligand interactions. *Biochemistry* **36**, 5837–5845.

Roy M, Brader ML, Lee RW-K, Kaarsholm NC, Hansen J, Dunn MF. 1989 Spectroscopic signatures of the T to R conformational transition in the insulin hexamer. *J Biol Chem* **264**, 19081–19085.

Seydoux F, Malhotra OP, Bernhard SA. 1974 Half-site reactivity. *CRC Crit Rev Biochem* **2**, 227–257.

Smith GD, Dodson GG. 1992a The structure of a rhombohedral R_6 insulin hexamer that binds phenol. *Biopolymers* **32**, 1749–1756.

Smith GD, Dodson GG. 1992b Structure of a rhombohedral R_6 insulin/phenol complex. *Proteins: Struct Funct Genet* **14**, 401–408.

Smith GD, Ciszak E, Magrum LA, Pangborn WA, Blessing RH. 2000 R_6 hexameric insulin complexed with *m*-cresol or resorcinol. *Acta Cryst* **D56**, 1541–1548.

Storm MC, Dunn MF. 1985 The Glu(B13) carboxylates of the insulin hexamer form a cage for Cd^{2+} and Ca^{2+} ions. *Biochemistry* **24**, 1749–1756.

Sudmeier JL, Bell SJ, Storm MC, Dunn MF. 1981 Cadmium-113 nuclear magnetic resonance studies of bovine insulin: Two-zinc insulin hexamer specifically binds calcium. *Science* **212**, 560–562.

Whittingham JL, Chaudhuri S, Dodson EJ, Moody PCE, Dodson GG. 1995 X-ray crystallographic studies on hexameric insulins in the presence of helix-stabilizing agents, thiocyanate, methylparaben, and phenol. *Biochemistry* **34**, 15553–15563.